European Journal of Molecular & Clinical Medicine
ISSN 2515-8260 Volume 07, Issue 07, 2020

Recent advances in MXene-based electrochemical sensors

Chirag Verma[1], Kamal Kishor Thakur[2]

[1]*Chiragverma976@gmail.com*

[1,2]*University Institute of Science, Chandigarh University.*

Abstract : MXene is another two dimensional material which is as of late found in 2011, it incorporates transition metal nitride and metal carbide. Mxene show different applications in fields like catalysis, detecting, clean energy, power devices, super capacitors and electronics. This review focuses on the research done on the electrochemical detecting properties of Titanium carbide MXene from year 2015- 2020, we have examined the electrochemical sensors fabricated by using $Ti_3C_2T_x$ for biomedical application, biomolecule detection and environmental monitoring.

Keywords: Titanium Carbide MXenes, Electrochemical (bio) sensors, Biomarker, Environmental pollutants

Introduction

2D materials are popular for their novel chemical, physical and electric properties. These properties 2D materials are suitable for energy storage, catalysis and electronic applications [1, 2]. Some of known two dimensional nanomaterials are graphene nanosheets and MoS2 nanomaterials. Recently another group of 2D materials have been found referred to as mxene, which contain transition metal nitrides, carbides and carbonitrides. MXene are first discovered in 2011 by researchers at Drexel University [3]. MXene are synthesized from MAX phase by a process of selective etching of A atomic layer, where M refers to early d-block transition metals, A is element from group 13 and 14 elements and X stands for Carbon or Nitrogen atoms [4]. The MAX phase is a firmly stuffed multilayer structure consisting of alternate atomic layers M and X, with solid M-X and weak M-A bonds in this max phase (Fig.1). The general formula for representing two dimensional MXenes is Mn+1XnTx, where T represents surface functional groups such as -OH, =O and –F and n are integers from 1,2,3……. Fig 1.

Mxene has recently drawn considerable interest from researchers due to their special layered morphology, enormous surface area, good thermal stability, high electric conductivity, excellent hydrophilicity and environmental friendly characteristics. These remarkable and amazing attributes of MXene makes them valuable for energy storage [5], catalysis [6], ecological remediation [7], and detecting purpose [8]. MXene have comparative properties to those of other 2D materials, for example, graphene, metal oxide(MO) etc. since mxene have better properties in this manner it could be a best option in comparison to other 2D materials. Mxene are made of non toxic elements and also their decomposed byproducts are non toxic therefore mxene could have number of applications in environmental remediation applications [7]. 2D materials such as MoS_2 and graphene [9,10] have been highly researched in past years for developing sensing instruments. However these 2D materials have a few downsides such as low electric conductivity, high hydrophilicity and trouble in surface

functionalization. MXene is good option in contrast to other 2D materials, since it has electric conductivity, high hydrophyllicity, good ion intercalation behavior and simple functionalization also mxene could be easily produced at large scale. All these properties are ideal for developing high performance electrochemical biosensors.

Synthesis

MXene are synthesized by etching of atomic layers A (of main group s and p elements) from MAX phases. MAX phase have hexagonal structures made out of MX (transition metal carbide or nitrides) layers which are held together by interleaved atomic A layer. To get 2D MXene from MAX phase, the removal of A atomic layer is essential step, which is not possible by physical methods because of strong M-A bond in MAX phase. Synthesis of MXene by exfoliation method is a top-down approach. Synthesis of MXene generally involves the breakage of large bulk precursors, these precursors are of two types first are Non-max phase precursors and second are max phase precursors [11]. Generally MAX phase precursors are used for mxene production due to their high efficiency [11]. By selective etching of Al layer, single layered MXene are obtained. In this process MAX phase is first treated with etching reagent and then followed by sonification to obtain single layer MXene [12,13]. MXene can be synthesized by two techniques, first involves the use of HF etchant and second involves non-HF etchant.. In HF etching method aqueous HF acid is used as etchant. The synthesis of mxene takes place three steps, chemical reaction between aqueous HF and MAX Ti_3AlC_2

1. $M_{n+1}AlX_n + 3HF \longrightarrow AlF_3 + M_{n+1}X_n + 1.5\ H_2$
2. $M_{n+1}X_n + 2H_2O \longrightarrow M_{n+1}X_n(OH_2) + H_2$
3. $M_{n+1}X_n + 2HF \longrightarrow M_{n+1}X_nF_2 + H_2$

Step 1 involve the removal of Al layer by the action of HF on max phase, in step 2 and 3 the surface termination of MXene surface takes place with F and OH groups. Ti-Al bond present in MAX phase breaks and new Ti-OH and Ti-F bonds are formed in reaction [14]. In this method HF concentration plays very significant role in the quality and quantity of MXene, high concentration of HF (>40% v/v) products well isolated layered structure with low crystalinity where as low concentration of HF don't deliver good morphology and accordion like shape [15]. Mxene synthesized by this method have multilayered structure and needed to be treated further to obtain single layer. To remove this problem new method are developed. This new method involve the use of non-HF etching, in this method HF is generated during the reaction by reacting acid with fluoride usually HCl and LiF mixture is used [11].

$$LiF(aq) + HCl(aq) \longrightarrow HF(aq) + LiCl(aq)$$

This method has some advantages over HF method some are high exfoliation yield, low sonification time, less defects, easy to handle and less hazardous [16]. After etching next step involve filteration and centrifugation of reaction mixture to get solid having accordion like loosely packed structure. Reaction mixture is centrifuged for 10 minutes so that solid product can settle down, after that solid product is collected and washed with double distilled water for 2-3 times until the pH of the product comes in the range of 4-6[17,18,19].

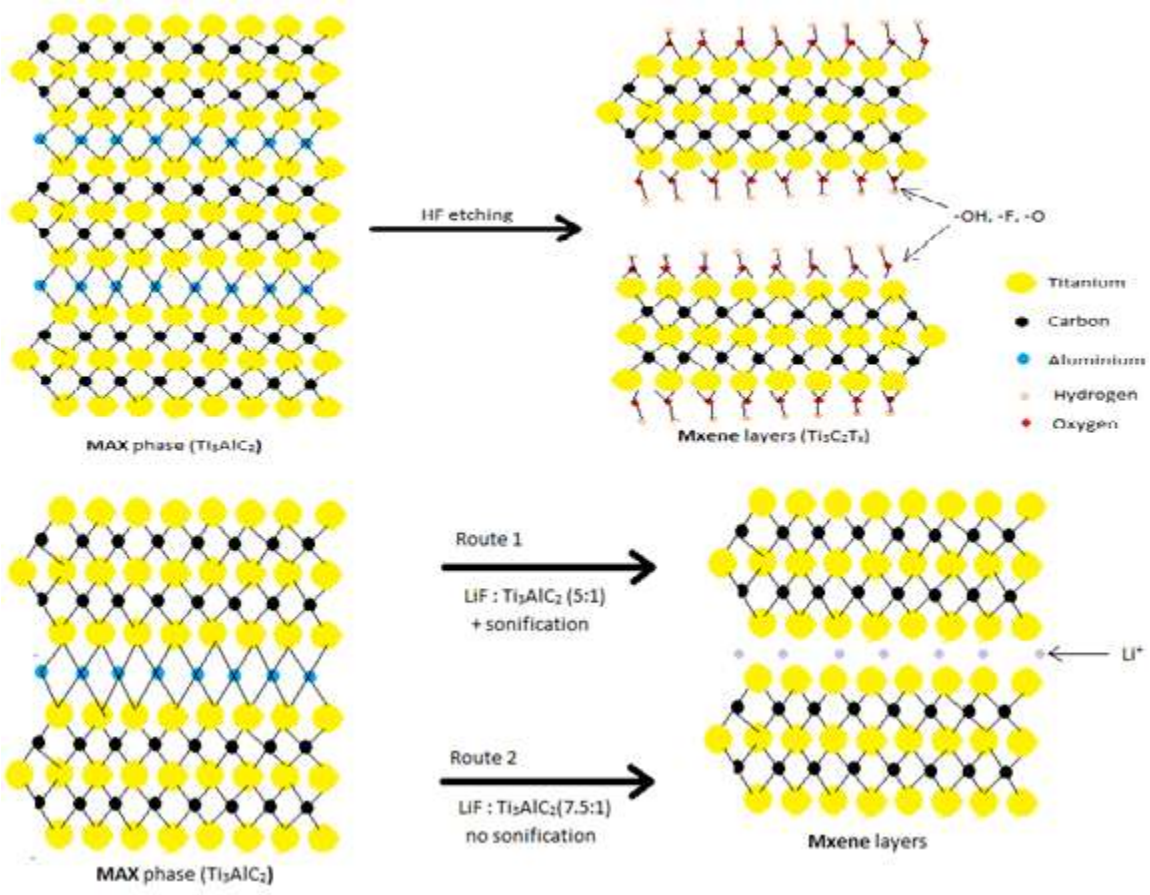

Fig.1. (a) Synthesis of MXene from MAX phase by using HF etchant. (b) Synthesis of MXene nanosheets through non-HF etching (generally hydrochloric acid and metal fluoride mixture is used) with and without sonification

Exfoliation and surface modification/functionalization

Mxene synthesized by HF etching have multilayered structure, these layers were held by weak vanderwall forces and hydrogen bonding. Single layer mxenes are obtained by delaminating multilayer mxene. Delamination is performed by using intercalating agents, these agents increases the interlayers distance by weakening the interlayer distance. There are two types of intercalant, organic intercalant and metal intercalants. These were added into the reaction mixture before sonification to exfoliate multilayer mxene. The first type of intercalants are metal ions such as metal halide salts and metal hydroxide in aqueous solution. For example when LiF/HCl is used for synthesis, Li^+ ions intercalate between the interlayers of Mxene. Second type of intercalant are organic molecules, generally polymeric organic molecules and ionic molecules are more effective intercalants. Dimethyl sulphoxide (DMSO) is very effective for $Ti_3C_2T_x$ mxene but can't be used for other mxene [20], isopropyl amine can be used for Nb_2CT_x, Nb_4C2Tx, $Ti_3C_2T_x$ [21]. Other intercalating agents are tetrabutylammoniumhydroxide(TBAOH), [22] tetramethylammoniumhydroxide(TMAOH) [23], and urea [24].

MXenes exists in the form of layers that provides it novel chemical, electrical, ion transport and physical properties, these novel properties are responsible for various applications of MXene material [25-27]. Due to high metallic conductivity and small band gap

characteristics, MXenes have good electrical conductivity, which makes it suitable for super capacitor and Li-ion battery applications etc. [28]

Mxene as sensors

The surface of MXene is tremendous which allows the functional groups to effectively immobilise on the surface. It has demonstrated considerable possibilities for sensing applications due to the high electric conduction and low electron transfer resistance. MXene can be used for biosensing applications because of its properties like novel morphology, enormous surface area, good electric conductivity, easy functionalization and biocompatibility. Electrodes based on MXene are effective transducers that deplete biological receptors on their surface and thus help to attain DET, high selectivity and sensitivity. The MXene based electrochemical luminescence sensor is designed to detect label-free single nucleotide mismatch in human urine sample. Ti3C2 becomes more negatively charged after terminating with OH groups which increases its electrical conductivity (such as 6500 S cm-1). Using MXene and Nafion the solid state Electrochemical Luminescence (ECL) sensor was developed. MXene provides good conduction capability for the composite film and increases $Ru(bpy)_3^{2+}$ adsorption on the surface of the electrode. An extremely low analyte concentration can be detected by this sensor which shows very low 5nM detection. The biosensor demonstrates outstanding reproducibility (RSD=0.69%) and good stability [29]. A titanium carbide composites based electrochemical sensor was developed for Dopamine (DP) detection in blood. $Ti_3C_2T_x$ nanosheets are stabilized with Nafion. Sensor shows excellent sensitivity, stability, selectivity and large detection range of 0.015-10 micro molar. This sensor is extremely sensitive to dopamine showing 3nM detection limit. This high biosensor sensitivity is due to strong electrical conductivity, low resistance to charge transfer and enormous surface area for successful functional group immobilization [30]. For gliotoxin identification, an electrochemical biosensor is generated based on DNA/MXene nanocomplexes. MXene provides medium for DNA immobilization which are integrated into MXene surface through interactions between titanium atoms and DNA phosphate groups. MXene ($Ti_3C_2T_x$) provides the biosensor both stability and good sensing ability. The tetrahedral DNA non-structure is used as a gliotoxin binding site and Pristine/Ti3C2Tx is used as an electrocatalyst for electrochemical sensing. For $Ti_3C_2T_x$/GCE and GCE, the charge transfer resistance is 616 and 898 ohm respectively, which show's that the resistance value of biosensor decreases when MXene material is used with GCE. Biosensor exhibit low LOD (5pM) and large detection range of 5pM to 10nM [31]. Mxene based electrochemical sensor for nitride detection have been documented by H. Liu et al. Here hemoglobin modified mxene nanocomposite is used for nitride detection. Mxene improved the electron transfer rate and hence increased the electric conductivity of biosensor, which results in immediate transfer of electron from Hb to electrode and hence increases the selectivity of biosensor for nitrite (NO_2). Biosensor shows very low detection limit (0.12 μM) and large detection range of 0.5 to 11800 μM [32]. Lorencova et al. reported an electrochemical sensor for hydrogen peroxide sensing. This mxene ($Ti_3C_2F_x$) based biosensor shows very high sensitivity for H_2O_2 with 0.7 nM detection limit. In another work Pt modified MXene nonocomposite are drop casted on GCE. This biosensor shows 448 nM detection limit and its senstivity is not compromised by the presence of other redox molecules [33, 34]. The development of an electrochemical sensor for adrenaline detection in blood was reported by S. Sankar et al. Biosensor was constructed with MXene/GCPE nanocomposite, which can detect adrenaline in presence of phosphate buffer at 7.4 pH with 99.2–100% sample recovery. This biosensor exhibits very low detection limit of 9.5nM [35]. D. song et al. fabricated mxene based electrochemical sensor for pesticides detection. MnO2/Mn3O4 microcuboids and Ti_3C_2

MXene/Au nanocomposites are used to build this biosensor. The sensor demonstrated a remarkable performance for methamidophos detection when optimal conditions are applied. Mxene has characteristics that improve the electron transfer rate while promoting electrochemical reaction, such as a high conductivity, wide area and high biocompatibility. Sensor offers 1.34×10^{-13} M detection limit and long 10^{-12} M to 10^{-6} M detection range [36]. An electrochemical carbendazine sensor was developed by J. Yang et al. Delaminated MXene nanosheets were deposited on GCE and fluorine terminated MXene ($Ti_3C_2T_x$) nanosheets improves the electrochemical sensing of biosensor for carbendazim [37]. S. Zhou et al. reported the fabrication MXene/polyoxometalate nanocomposite for osteopontin (OPN) detection. $Ti_3C_2T_x$ MXene is modoified with polypyrrole to form $Ti_3C_2T_x$/polyoxometalate nanohybrid and composed with $Ti4^+$ and $Mo4^+$ ions (integrated with graphene sheets). After that OPN-targeted aptamer strands were immoblized on PPy@ $Ti_3C_2T_x$ /PMo nanohybrid. The biosensor presents ultra-sensitive detection with low LOD (0.98 fg/ml) and long detection range (0.05 pg/ml to 10.0 ng/mL) [38]. The MXene based electrochemical sensor was manufactured by depositing Nafion/$Ti_3C_2T_x$ composite on GCE for Bromate (BrO_3) detection in water. The biosensor showed wide detection range (50 nM-5 μM) and low LOD (41nM) [39]. S. Sun et al. modified $Ti_3C_2T_x$ mxene sheets with $W_{18}O_{49}$ nanorods to fabricate an electrochemical biosensor for acetone detection. $W_{18}O_{49}$ nanorods (NRs) were homogeneously deposited on mxene nanosheets by solvothermal process. The biosensor exhibits high acetone sensitivity having very low detection limit, i.e. 170 ppb, and a wide 11.6 to 20 ppm detection range. The biosensors showed high sensitivity because of the homogeneous distribution of W18O49 nanorods (NRs) over MXene surface [40]. R. Huang et al. designed MXene based electrochemical sensor to detect hydroquinone (HQ) and catechol (CT) in industrial waste water. The biosensor was built by depositing MWCNTs on MXene nanosheets. The detection limit of this biosensor is 6.6 nM for HQ and 3.9 nM for CT which is very low and has a large detection range of 2 - 140 μM [41]. Mxene based electrochemical sensor was fabricated by J. Jiang et al. for the detection of organophosphate pesticides. Ag@ $Ti_3C_2T_x$ nanocomposites are fabricated by Ag metal reduction with MXenes, followed by acetyl cholinesterase (AChE) immobilization on the surface of MXene. Malathion was detected by this electrochemical sensor in the 10^{-14} - 10^{-8} M concentration range. Biosensor works on enzymatic inhibition pathway principle [42]. R. B. Rakhi et al. fabricated Au/MXene based biosensor for glucose detection. The electrochemical biosensor is very sensitive for glucose which is due to the presence of glucose oxidase. Biosensor GOx/Au/MXene/Nafion/GCE shows a very low 5.9μM detection limit. Au nanoparticles improve the electrical conductivity of the composite, and Nafion also reduces the interfering signals because of its –ve charged polyelectrolyte matrix [43]. P. Rasheed et al. reported a mxene based electrochemical sensor for L-cysteine (L-Cys) detection, which was synthesized by modifying MXene with Pd nanoparticles (NPs). This sensor exhibits a very low LOD (0.14mM) and large detection range (0.5 - 10mM) [44]. H. Tai et al. fabricated TiO_2/ $Ti_3C_2T_x$ MXene based electrochemical sensor detecting NH_3 gas. This bilayer $TiO_2/Ti_3C_2T_x$ nanoomposite was fabricated by mixing TiO_2 with mxene nanosheets, which increased its sensing properties. The $TiO_2/Ti_3C_2T_x$ sensor reacts to very low ammonia concentrations (0.5 ppm) and has a wide detection range of 2-10 ppm. [45]. F. Zhao et al. fabricated electrochemical biosensor by altering 2D MXene nanocomposites with Au-Pd nanoparticles. Au-Pd nanoparticles have improved catalytic efficiency and serve as a tool for the immobilization of acetyl cholinesterase. This biosensor is very sensitive to organophosphorous pesticides and has a low 1.75 ng L-1 detection limit and large detection range (0.1 - 1000 μg/L).

Mxene based electrochemical (bio) sensor

This section covers sensing applications for the identification of medicinal agents, environmental toxins and biomarkers with electrochemical sensors based on MXene. All the processes of synthesis, electrochemical responses of nanocomposite are discussed briefly. The purpose of this review is to highlight the advancements in electrochemical properties (sensitivity, stability, selectivity, detection range, detection limit etc.) of MXene nanocomposites. Table 1 summarizes the MXene-based sensors for different types of detection.

1. **Detection of biomarkers**

According to a report of National Cancer Institute (NCI), biomarkers are very important biological molecules which are present in the blood and tissues. These biomolecules can be recognized as an indication of typical/anomalous biological processes and pathogenic conditions / infections. Therefore the detection of these biomarkers can become an important step in the clinical field for early finding of diseases and risk assessment. This increases the possibility of effective and rapid treatment, and therefore it can increase the life. These biomarkers can be detected in tissue samples and body fluids (blood, urine) in a non-invasive way. In recent years electrochemical sensors has shown various possibilities for biomolecule detection, hence electrochemical bio sensors may be a reliable option for non invasive measurements.

MXene based sensor for the detection of breast cancer biomarker Mucin1

Mucin1 is identified as a biomarker because of its irregular presence in tumor tissues. In breast cancer patients MUC1 is highly expressed as compared to normal people [47]. Therefore, it becomes very important to detect MUC1 for the early diagnosis. H. Wang et al. reported the development of electrochemical bio sensor for detecting breast cancer biomarker Mucin1 [48]. In this work MXene nanosheets (Ti3C2) were used for fabricating electrochemical biosensor. Ferrocene-labeled DNA was first bounded on MXene surface to fabricate cDNA-Fc/MXene probe. After that AuNPs were electrodeposited using the chronoamperometry process on GCE surface And then MUC1 aptamer was fixed on electrode surface through Au-S bonding to fabricate Apt/Au/GCE electrode. After that Apt/Au/GCE was immersed in cDNAFc/MXene solution and washed with PBS buffer solution. Thus the developed electrochemical aptasensor cDNA-Fc/MXene/Apt/Au/GCE was utilized for MUC1 detection.

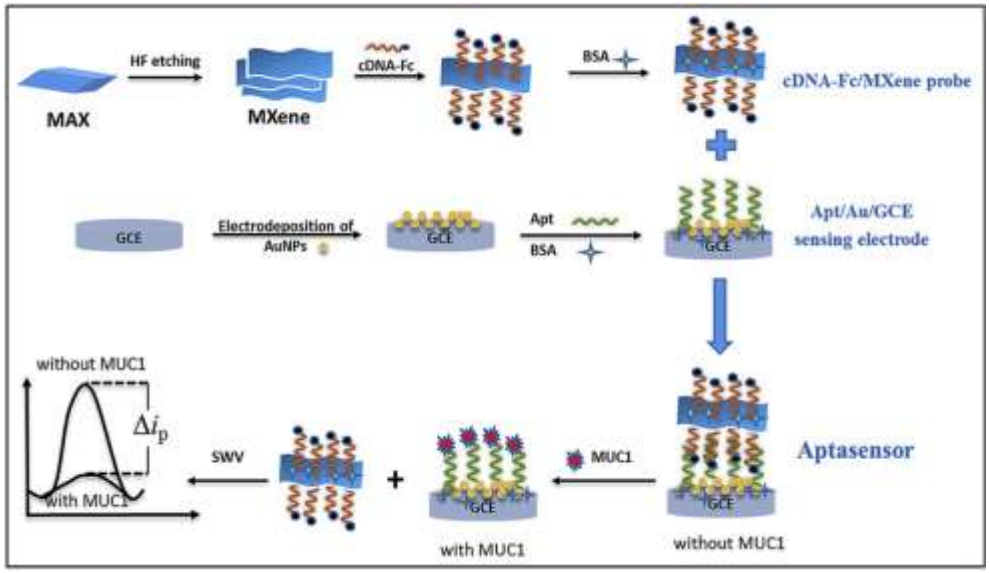

Fig.2. Schematic representation of the manufacture procedure of electrochemical aptasensor for identification of cancer marker MUC1. Reprinted by permission from Ref. [48]. Copyright 2020, Elsevier.

In Fig.3 the EIS spectra of modified electrode and bare Glassy Carbon Electrode are given, where curve a and b are for bare GCE and AuNPs modified electrode respectively, modified electrode has relatively small semicircle as compared to bare GCE, because of the higher conductivity of AuNPs which accelerated the electron transfer rate. After modifying Au/GCE with Apt, the size of the semicircle increases significantly this increase in size is due to the nonconductive nature of Aptamer (curve c). The curve d showed that the size of the semicircle continued to increase as the cDNA-Fc/MXene probe was deposited on Apt/Au/GCE. When sensor was used for MUC1 sensing, a process occurs between cDNAferrocene/MXene and MUC1 probes, in this process mxene probe detaches from electrode, which decreases the electrical signal of sensor. The binding of biomarker with Aptamer facilitate the release of probe which was confirmed by decrease in semicircle diameter shown by curve e. These changes in peak current height, before and after the detection are utilized to detect MUC1. The biosensor shows large detection range (1 pM to 10 µM), low detection limit (0.33 pM), 99.0-100.2% recovery, and 1.23-6.16% RSD in serum samples.

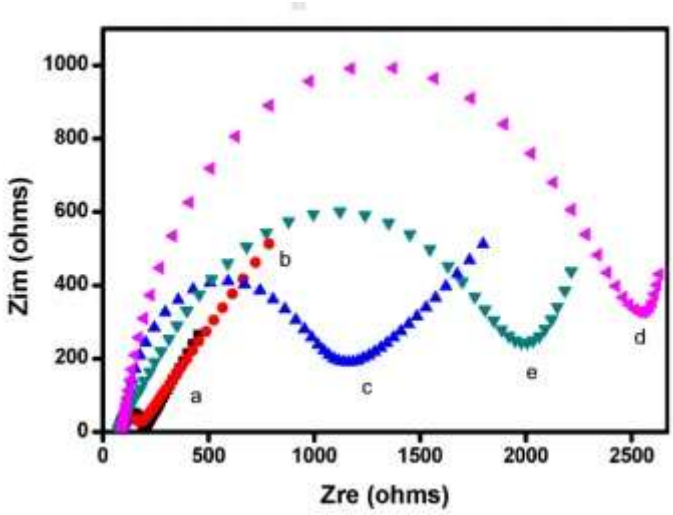

Fig.3. EIS spectra of different electrodes (a) GCE, (b) Au/GCE, (c) Apt/Au/GCE, (d) cDNAFc/MXene/Apt/Au/GCE and (e) MUC1/Apt/Au/GCE. Reprinted by permission from Ref. [48]. Copyright 2020, Elsevier.

D. fang et al. reported MXenes based dual-mode probe for exosomes sensing in which black phosphorus quantum dots were deposited on mxene surface [49]. Ti_3C_2 MXene was first synthesized using HF etchant and then the ECL bioprobe (MXenes-BPQDs@Ru(dcbpy)$_3^{2+}$-PEIAb$_{CD63}$) was created. BPQD's catalysed the electrochemical oxidation of Ru(dcbpy)$^{2+}_3$ and enhanced ECL signal. This enhancement in ECL signal was due to the electrochemical nature of BPQD. BPQD acts as coreactant of luminophore Ru(dcbpy)$^{2+}_3$ and improves ECL emission. Ru(dcbpy)$^{2+}_3$ - BPQD composite was deposited on GCE and a much higher ECL signal was obtained because of the shortening of electron transfer distance among luminophore and coreactant. MXene-BPQD nanocomposites have a major impact on amplifying the ECL signal because of unique electronic properties of both MXene and BPQD. MXene have excellent metallic conductivity and BPQD exhibit unique electronic properties due to their ultra small size. Then GCE was modified with SiO_2 nanourchin (NU's), after that Ionic liquid was dropped onto SiO_2 NU's/GCE, followed by aptamer deposition on modified electrode followed by incubation for 40 minutes. Then exosomes are deposited on modified electrode. At last the fabricated ELC bioprobe was dropped on modified electrode (exosome/Apt/ILs/SiO_2NU's/GCE) and allowed to incubate for 50 days. The obtained ECLprobe/exosome/Apt/ILs/SiO_2NU's/GCE biosensor was stored at 4 °C for reuse. ECL biosensor has excellent sensitivity for exosome, it has very low detection limit of 37particle/μL. It exhibited wide detection range (1.1×10^2 to 1.1×10^7 particle/μL) and 96 to 106 precent recovery for HCF-7 and Hela cells.

MXene based biosensor for the detection of Mycobacterium tuberculosis bio marker

J. Zhang et al. reported the development of MXene (Ti_3C_2) based electrochemical sensor for Mycobacterium tuberculosis detection [50]. Electrochemical sensor is made of two parts one is capture probe and second as signal amplifier transduction material, acts as capture probe to bind with target biomarker (16S rDNA fragments for M. tuberculosis) and MXene acts as signal amplifier transduction material. Mxene has hydrophilic nature, high conductivity and large surface area, mxene can interact with huge number of bio molecules due to its hydroxyl, and oxygen terminated surfaces and enormous surface area. When certain fragments of 16S

rDNA of M. tuberculosis are present in the sample, hybridization takes place between target and PNA probe, which exposes a large no of phosphate anchoring sites of target biomolecule to sensing surface of electrode. Therefore zirconium cross connected Ti_3C_2 MXene can connect directly to the phosphate group and close the gap between the disrupted AuNPs at the network electrode. It results in a change in the conductance of the electrode and confirms the detection of M. tuberculosis. Sensor exhibits low detection limit (LOD) of 20CFUml^{-1}. Biosensor exhibits high sensitivity and specificity of 91.7% and 89.3% respectively. The reported biosensor takes 2h to show the result as compared to the traditional culture method which require 21 days to obtain results. The proposed biosensor was faster, simpler, less expensive, has wider linear detection range and and higher sensitivity compared to other techniques.

Sensor for Acetone

Acetone is very important biomarker for diabetes, acetone sensors are used to detect acetone concentration in human breath. It is viewed as basic marker for the analysis of patients with diabetes. S.Sun et al. reported the construction of W18O49/Ti3C2Tx nanocomposites for acetone gas sensing [51]. Mxene is a 2D substance with possible applications for gas sensors and biosensors. The functional groups present at the surface of mxene can serve effectively as active gas adsorption sites. Tungsten oxide ($WO_{x\leq3}$) has outstanding chemical stability, low cost, fast synthesis and diversity of structure. They have several vacancies for oxygen, which function as additional active gas adsorption sites. Tungsten oxide has excellent chemical stability, low cost, easy synthesis and structural diversity. To improve the sensing activity, $WO_{x\leq3}$/mxene based nano-composite was fabricated which acts as very sensitive platform for acetone gas sensing. Sensor exhibits low detection limit of 170ppb acetone. Mxene sheets acts as templates for anchoring $WO_{x\leq3}$ nano rods. $W_{18}O_{49}/Ti_3C_2T_x$ nano-composite is made using a solvothermal facile method. $W_{18}O_{49}/Ti_3C_2T_x$ nanocomposites showed huge enhancement for acetone sensing compared to $W_{18}O_{49}$ nano rods and $Ti_3C_2T_x$ Mxene sheets. Sensor exhibited high sensitivity, selectivity, stability, high response for low concentration, rapid response and very low detection limit (170ppb).

2. **MXene based sensor for pharmaceutical**

MXenes has also been used for the delicate characterization of therapeutic agents in addition to the analysis of biomarkers. In this part, we audit the new advancement in the use of MXene for electrochemical detecting of remedial compounds. The most alluring properties of MXenes are high surface area, high electrical conductivity, 2D layered morphology, hydrophilicity and biocompatibility which are utilized with different nanomaterials for electrochemical detection. Conventional detection methods namely mass spectrometry, chromatography, and immunoassay are heavily burdened with difficult instrumentation, high analysis costs, and many sample preparation measures that delay the availability of test results. In contrast, nanomaterial based electrochemical (bio) sensors are designed with excellent sensitivity, selectivity, rapid detection, and more flexible design [52, 53]. Kalambate et al. fabricated MXene/MWCNT/chitosan electrochemical sensor to detect sumatriptan(SUM), ifosfamide(IFO), acetaaminophene(ACOP) and domperidone(DMO) [54]. By selectively etching the Al layer using aqueous HF, Ti3C2 MXene was synthesized from the max phase, after that Ti_3C_2 MXene and MWCNT were added to chitosan solution and mixture was ultrasonicated. After sonification the suspension of Ti_3C_2/MWCNT's/chit was drop casted on GCE and thus Ti_3C_2/MWCNT's/chit/GCE electrode was obtained. MXene show excellent electronic conductivity which makes it suitable for electrochemical

applications. Mxene shows well separate accordion like structure (fig. 4b), Mxene nanosheets provides large surface area for MWCNT's entrapment and offer sufficient space for MWCNT deposition on the surface and also on interlayers of mxene.(fig1c.) MWCNT acts as separator and bridges the gap between Ti_3C_2 interlayers and produces a conductive network. The occurrence of C, Ti, O, F in nanocomposites is verified by XPS spectra of Ti_3C_2 and the active etching of the Al layer from Ti_3AlC_2 is also confirmed. XPS spectra of Ti_3C_2 and Ti_3C_2/MWCNT confirmed the occurrence of C, Ti, O, F elements while intensity of C 1s is high for Ti_3C_2 /MWCNT which ensures the presence of MWCNT (fig 5a). Electrochemical studies of MXene/MWCNT's/chit/GCE electrode are performed to test its selectivity and sensitivity.

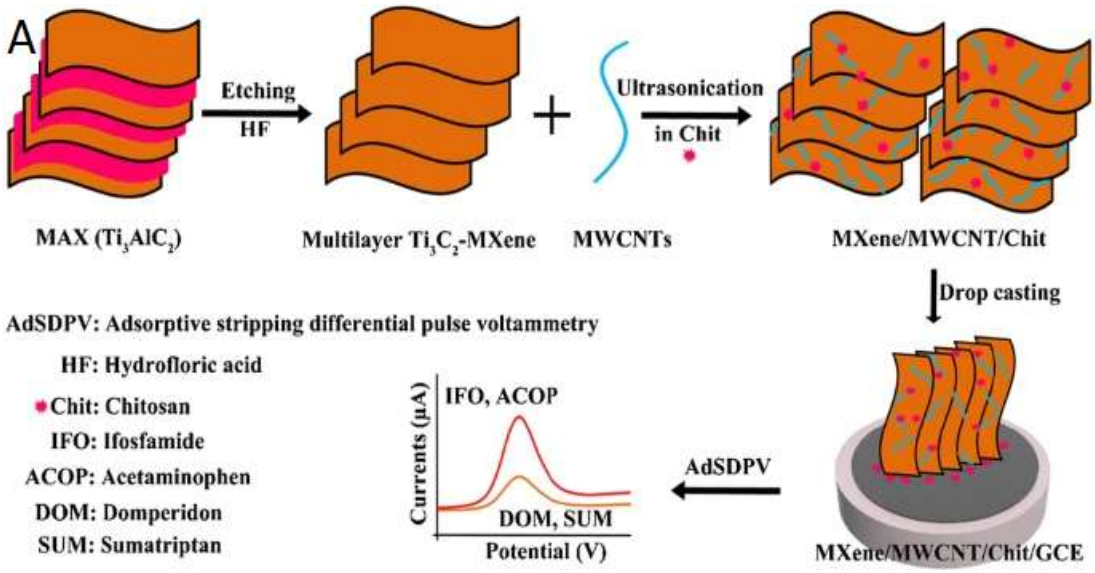

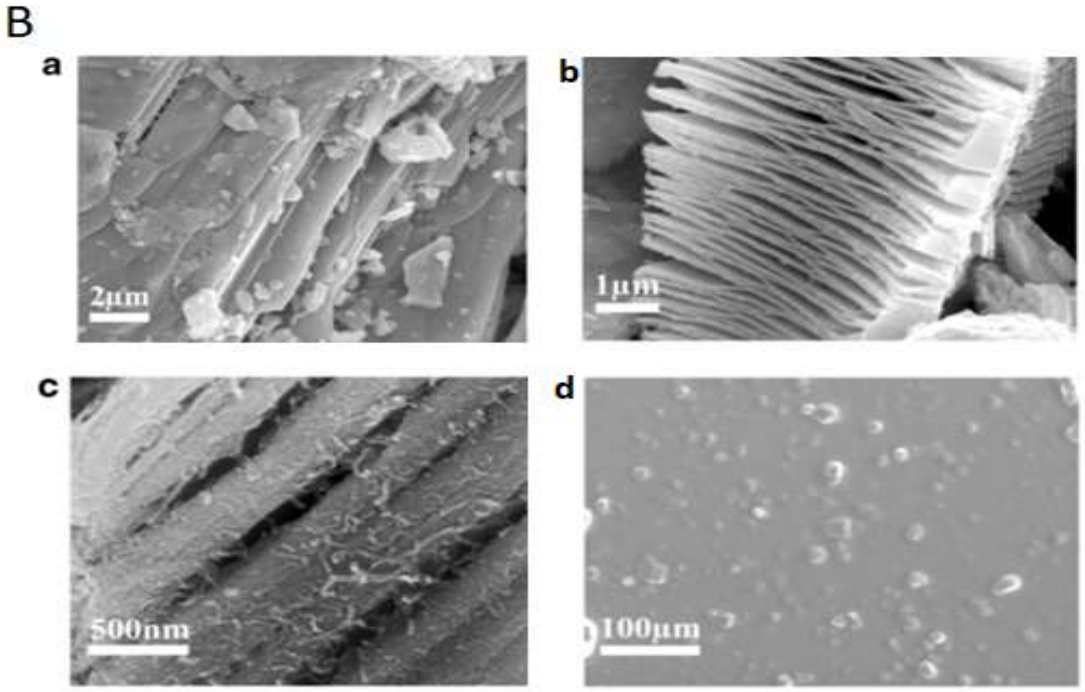

Fig.4. (A)Schematic demonstration of Ti3C2 MXene and Ti3C2/MWCNT/Chit nanocomposite synthesis process. (b) SEM images of Ti3AlC2 (a) before and (b) after treatment with HF; SEM images of (c) Ti3C2/MWCNT low magnification (d) Ti3C2/MWCNT/Chit composite. Reprinted by permission from Ref. [54]. Copyright 2020, Springer Nature.

CV response of changed electrode demonstrated well outlined redox peaks (fig. 5b) of $[Fe(CN)_6]^{3-}$ complex. The peak current of Ti3C2/MWCNT/chit/GCE is greater than Ti3C2/GCE but less than Ti3C2/MWCNT's/GCE, which is because of insulating nature of chit. Redox peak current proportion (I_{pc}/I_{pa}) of uncovered GCE, Ti_3C_2/GCE, MWCNT's/GCE and Ti_3C_2/MWCNT's/chit/GCE are 0.752, 0.89, 0.921, 0.964 respectively. The active surface area was 0.024cm2, 0.035 cm2, 0.044 cm2 for GCE, Ti3C2/GCE and Ti3C2/MWCNT/chit/GCE. The effective area of Ti_3C_2/MWCNT's/chit/GCE was 1.83 times higher compared with bare GCE, this confirms the enhanced electric conductivity of Ti_3C_2/MWCNT's/chit/GCE nanocomposites. In the modified electrode/electrolyte interface, the EIS analysis demonstrated electrochemical interfacial properties. Fig. 5c showed the Nyquist plots of GCE, Ti_3C_2/GCE and Ti_3C_2/MWCNT's/chit/GCE, these plots showed large semicircle for GCE which decreases considerably upon modification with Ti_3C_2 and Ti_3C_2/MWCNT's/chit nanocomposites. R_{ct}(charge transfer resistance) value of GCE, Ti_3C_2/GCE and Ti_3C_2/MWCNT's/chit/GCE are 1.53, 1.04 and 0.69 kΩ, respectively which confirms enhanced electron transfer kinetics at electrode/electrolyte interface. Fig. 5d-g shows the CV plots of IFO, DOM, SUM and AOCP on GCE, Ti_3C_2/GCE and Ti_3C_2/MWCNT's/chit/GCE electrodes. The oxidation peaks of these analyte are more intense at Ti_3C_2/MWCNT's/chit/GCE electrode as compared to Ti_3C_2/GCE and bare GCE, which is due to the high electron transfer rate of modified Ti_3C_2/MWCNT's/chit/GCE electrode. Oxidation process of these molecules (IFO, SUM, DOM) is irreversible confirmed by the absence of reduction peaks for these molecules, except AOCP which showed less intense reduction peak indicating its quasi reversible behavior. CV plots show that the oxidation peak current for each analyte was high on modified electrode as compared to bare GCE.

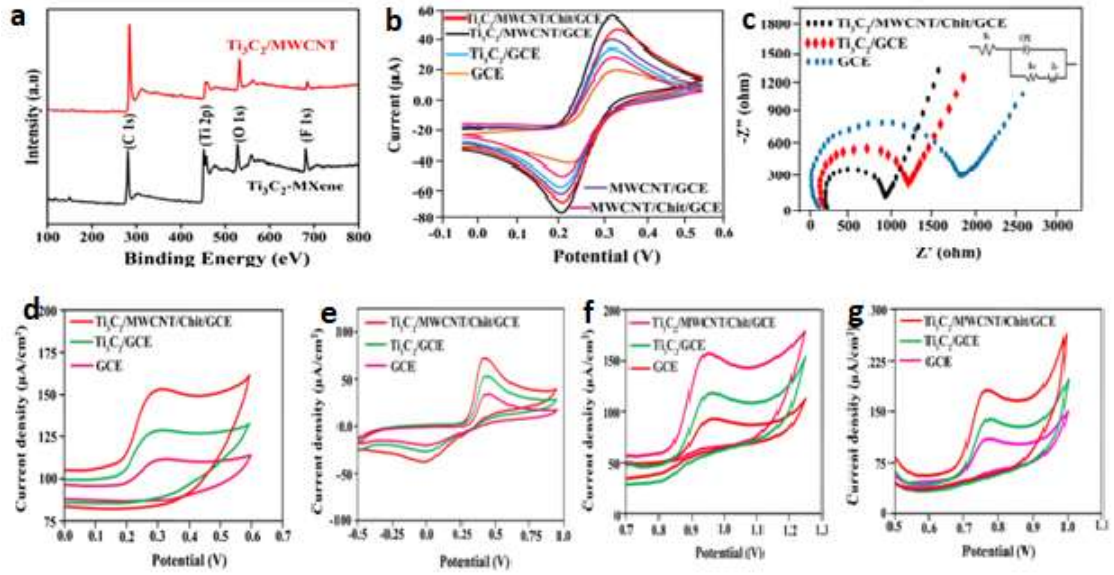

Fig.5 (a) XPS spectra of Ti3C2 and Ti3C2/MWCNT (b) Cyclic voltammograms and(c) Nyquist plots of GCE, Ti3C2/ GCE, Ti3C2/MWCNT/GCE, and Ti3C2/MWCNT/Chit/GCE. Cyclic voltammogram of IFO (d), ACOP (e), DOM (f), SUM (g) on the surface of these electrodes. Reprinted by the permission from Ref. [54],Copyright 2020, Springer Nature.

The synergistic effect of Ti_3C_2 mxene and conducting MWCNT's has enhanced the sensitivity of sensor, enhanced electrochemical reaction and electrode kinetics at electrode surface. This biosensor was used for analyte analysis in blood and urine samples. Biosensor has effectively detected DOM, IFO, SUM, and ACOP in the concentration range 0.0046–7.3, 0.0011–1.0, 0.0033–61, and 0.0042–7.1μM with low LOD of 0.00034, 0.00031, 0.00042 and 0.00028 μM respectively. This sensor showed high sensitivity for four analyte and response do not change in the presence of interferences like chemical species/drugs and metal ions. The sensor was highly stable and its stability was investigated for 60 days, it showed no change in response for first 20 days after 20days response started to deteriorate slowly. Only a loss of 4.1% and 9.2% was observed in AdSDPV signal after 30 and 60 days respectively.

3. **MXene based sensor for Environmental contaminants**

Ying He et al. constructed Bismuth/Mxene nanocomposite based electrochemical sensor to detect Pb and Cd [55]. Ions reminiscent of lead Pb, Cr, Cd and Hg are referred to as heavy metal ions, which don't degrade for quite a long time or even hundreds of years. This can contribute to numerous human health and other ecosystem diseases [56]. Likewise, these ions in the climate are exceptionally harmful and we have to eliminate them before accumulation [57-59]. A couple of techniques are used for detection of these particles including XRF, ICP-OES, AAS and ICP-MS are utilized for testing of these particles, however these procedures have restricted applications because of their significant expense and require trained individuals to operate hardware. It is therefore important to establish easy and affordable methods for detecting these ions. BiNPs/Ti_3C_2 nano-composites are synthesized by incorporating bismuth nanoparticles into thin sheets. MXene possess excellent electric conductivity, hydrophilic nature, large surface area, and chemical stability. Therefore it provides enormous surface area for the deposition of bismuth NPs over its surface. Bismuth nanoparticle has excellent electro analytical and catalytic activity. BiNPs were deposited over mxene sheets to obtain BiNPs/Ti_3C_2 nanocomposite. A homogeneous suspension of BiNPs/Ti_3C_2 nanocomposite was dropcasted on the GCE to get BiNPs/Ti_3C_2/GCE sensor. Fig. 6A shows CV polts for bare GCE, Ti_3C_2/GCE and BiNPs/Ti_3C_2/GCE. Three major oxidation peak currents are shown at 53.6, 130.5 and 162.9 μA for GCE, Ti_3C_2/GCE and BiNPs/Ti_3C_2/GCE. These results confirm the excellent electric conductivity of BiNPs/Ti_3C_2 nanocomposite. EIS plots of modified electrode (fig. 6B) showed the interfacial electron transfer resistance value (Ret) of 1500U, 720U and 450U on bare GCE, Ti_3C_2/GCE and BiNPs/Ti_3C_2/GCE were obtained. The low Ret value of BiNPs/Ti_3C_2/GCE is responsible for high electric conductivity of electrode. Cyclic voltagram was performed on GCE, Ti_3C_2/GCE and BiNPs/Ti_3C_2/GCE. In CV plots (fig. 6C) BiNPs/Ti_3C_2/GCE exhibit well characterized individual voltametric peaks at -0.57V (for Pb^{2+}) and -0.78V(for Cd^{2+}) as compared to bare GCE and Ti_3C_2/GCE. Biosensor has very low detection limit of 12.4 nm for Cd^{2+} and 10.8 nm for Pb^{2+}.

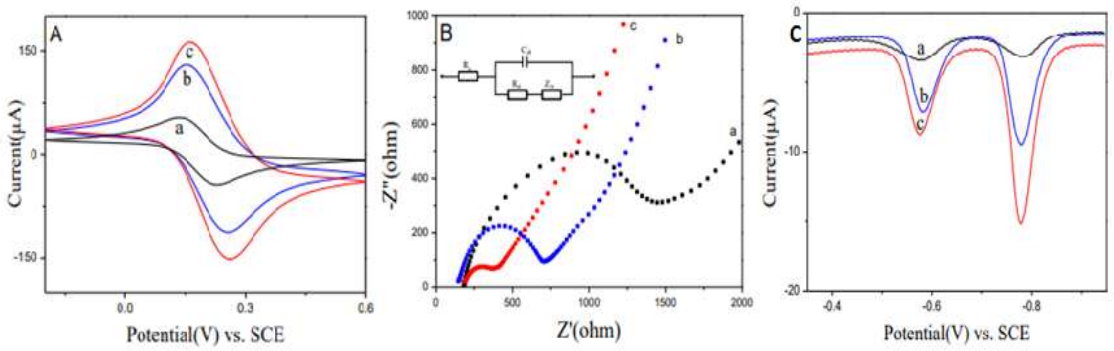

Fig.6. (A) Cyclic Voltammograms of plain GCE (a), Ti_3C_2Tx/GCE (b) and BiNPs@ Ti_3C_2Tx/GCE(c); (B) EIS spectra of plain GCE (a), Ti3C2Tx/GCE (b) and BiNPs@Ti3C2Tx/GCE (c); (C) SWASV curves of Pb^{2+} and Cd^{2+} at GCE (a), Ti3C2Tx/GCE (b) and BiNPs@Ti3C2Tx/GCE (c). Reprinted by permission form Ref. [55]. Copyright 2020, Nanomaterials.

Biosensor was highly selective for Cd^{2+} and Pb^{2+} ions and no significant interference was obtained with other metal ions expect Cu^{2+}, a little change in response signal was obtained when Cu^{2+} ions are present due to the creation of inter metallic compounds. The interference caused by Cu^{2+} can be avoided by adding ferro cyanide to analyte sample. Biosensor showed high stability and sensitivity of 95.2% (Pb^{2+}) and 94.5% (Cd^{2+}) after six weeks. In lake water and tap water samples, heavy metal ions were found with 98.3 percent recovery (Cd^{2+}) and 101.2 percent (Pb^{2+}) in tap water, while 101.5 percent (Cd^{2+}) and 106.3 percent (Pb^{2+}) in lake water were detected.

R. Huang, et al. reported Ti_3C_2/MWCNTs modified GCE electrode for detecting hydroquinone (HQ) and catechol (CT) [65]. Hydroquinone (HQ) and catechol (CT) show a high degree of biological and ecological toxicity. However, it is still a great challenge to detect them all at once due to interference from other chemical species. Therefore, various other techniques, such as mass spectrometry, liquid chromatography, HPLC and electrochemical methods have been developed to detect HQ and CT. Among these approaches, the electrochemical process has gained considerable attention in recent years, which are credited to cost-effective, simple, time-saving, high sensitivity and rapid response. Ti_3C_2-MXene was synthesized by using HCl and LiF mixture as etchant through selective etching of aluminum layer from Ti3AlC2 MAX phase. MWCNTs were deposited on Mxene sheets by a facile casting method to synthesis Ti3C2 based MWCNTs sensor. Then GCE was modified with Ti_3C_2-MWCNTs to obtain Ti_3C_2-MWCNTs/GCE.

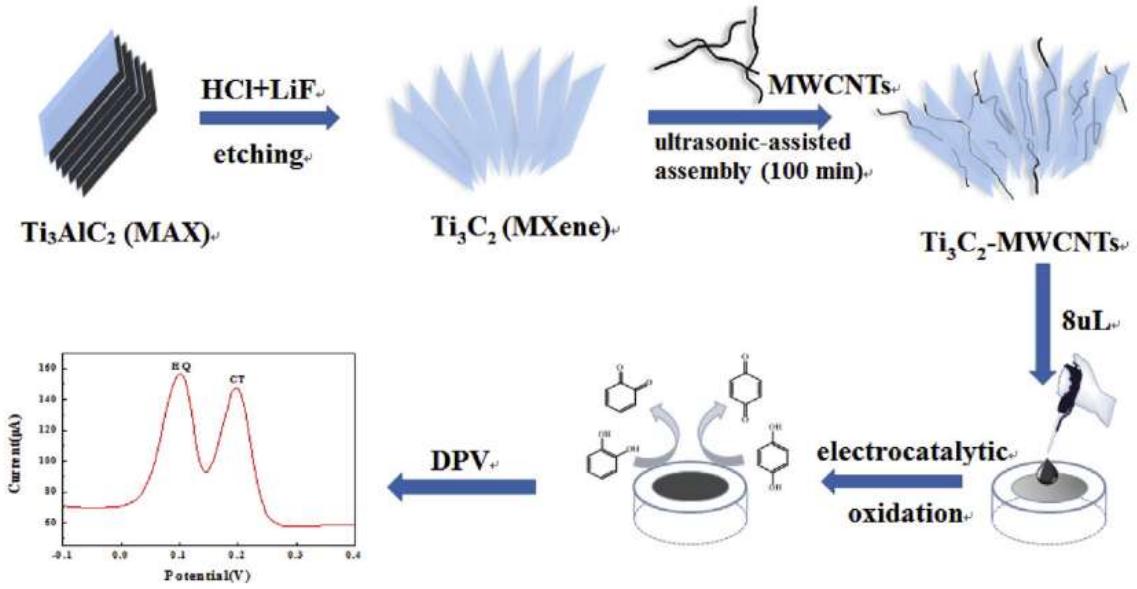

Fig.7. Schematic representation of synthesis process of Ti3C2-MWCNTs nanocomposite for detecting HQ and CT. Reprinted by permission from Ref. [65] Copyright 2019, Elsevier.

Cyclic Voltagram was performed to find the catalytic ability of bare GCE, MWCNTs/GCE, Ti_3C_2/GCE and Ti_3C_2-MWCNTs/GCE. CV responses for Ti3C2 / GCE, MWCNTs / GCE and Ti3C2-MWCNTs / GCE are better than simple GCE. Among all electrodes Ti_3C_2-MWCNTs/GCE showed best results because the conductivity of Ti_3C_2/MWCNTs nanocomposite is high due to the combination of Ti_3C_2 and MWCNTs metallic conductivity and excellent electroconductibility.

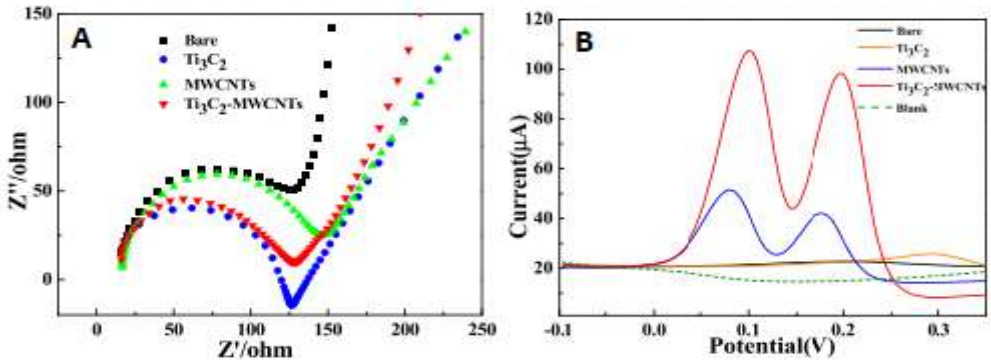

Fig.8. (A) Nyquist plots of Ti3C2/GCE, MWCNTs/GCE, bare GCE and Ti3C2-MWCNTs/GCE) (B) DPV response of Ti3C2/GCE, MWCNTs/GCE, bare GCE and Ti3C2-MWCNTs/GCE within the presence and absence of HQ and CT. Reprinted with permission from Ref. [65] Copyright 2019, Elsevier.

The Nyquist plot of Ti_3C_2/GCE, Bare GCE, MWCNTs/GCE and Ti_3C_2-MWCNTs/GCE is seen in fig.8A. The semicircle diameter is highest owing to its higher resistance in the case of bare GCE. The Rct value is 104.8 Ω and 119.1 Ω for MWCNTs/GCE and Ti_3C_2/GCE respectively which is relatively smaller compared to bare GCE (130.6 Ω). Fig. 8B illustrates DPV responses of HQ and CT on Ti3C2-MWCNTs/GCE, MWCNTs/GCE, Ti3C2/GCE and GCE. Bare GCE showed poor sensitivity toward HQ and CT while Ti_3C_2-MWCNTs/GCE

and MWCNTs/GCE could separate HQ and CT with a potential gap of 100 mV entirely. As compared to MWCNTs/GCE, Ti_3C_2-MWCNTs/GCE showed a far higher peak current that was 5.7 fold higher than MWCNTs/GCE. The DPV response to HQ and CT on Ti3C2-MWCNTs/GCE has been shown in figure 9(A) and (B). The biosensor exhibits a wide detection range and low LOD 6.6nM and 3.9nM for HQ and CT respectively.

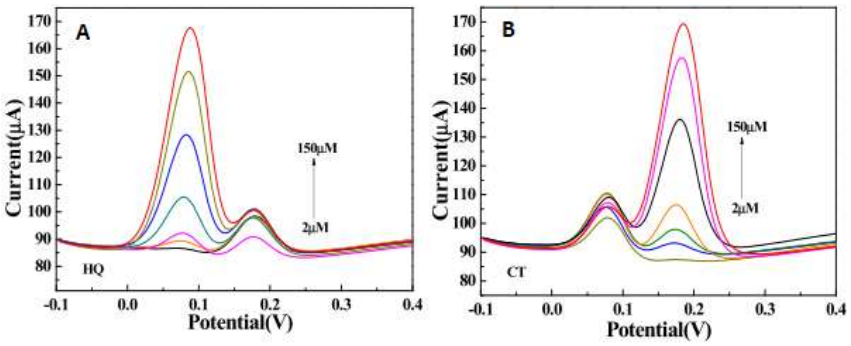

Fig.9. DPV responses of HQ(A) and CT(B) at various concentrations (2, 5, 10, 20, 50, 100, 150 μM) in the presence of 20 μM CT and 20 μM HQ respectively. Reprinted by permission from Ref. [65] Copyright 2019, Elsevier.

The Biosensor affectability don't change for HQ and CT within the sight of disruptive ions such as some inorganic ions ($Al^{3+,}$ Cu^{2+}, K^+, NO_3^-, Cl^-, Na^+, Mg^{2+}, Zn^{2+}, Ca^{2+}) and organic molecules for example paranitrophenol (p-NP), glucose (Glc), ascorbic acid (AA), resorcinol (Re), bisphenol A (BPA) which showed the outstanding selectivity and anti-interference characteristics of Ti_3C_2-MWCNTs/GCE. Sensor showed 96.9%-104.7% (HQ) and 93.1%-109.9% (CT) recovery in industrial waste water sample.

F. Zhao et al. reported the production of bimetallic/MXene nanocomposite for pesticide sensing [66]. Pesticides are significant environmental toxins and because of their over-use, can pose a severe threat to the health of both human and animal animals. Organophosphorus pesticides (OPs) are widely used pesticides that are primarily used to combat pest, parasitic weeds and plant diseases [67-69]. Although some of the most dangerous OPs have been supplanted by biodegradable chemicals, but the environment and agricultural goods do have problems caused by their residues. In addition some OPs can get oxidized and forms more toxic pesticides. For instance, in the atmosphere, parathion is eventually oxidized into paraoxon [70, 71] and its toxicity can pose significant risks to public health than that of the original compounds. Therefore the establishment of easy and local analysis methods for OPs and their derivatives is very important. Electrochemical biosensors are commonly used for quick and sensitive identification of pesticides as a general method of research. To detect paraoxon, a highly toxic organophosphorus pesticide, a mxene-based electrochemical sensor was developed in this research. Bimetallic nanoparticles provide promising feature for pesticide detection due to their good catalytic capacity and high specific surface area. In this work Au-Pd NPs are prepared on MXene ($Ti_3C_2T_x$) nanosheets surface by self-reduction process. After that the suspension of MXene/Au-Pd nanocomposite was drop casted on electrode (SPE) surface. MXene/Au-Pd nanocomposites show high conductivity and stability that enhances the electron transfer rate. This sensor has a very low 6.36 pM detection limit and large detection range. The fabricated biosensor selectivity was investigated for paraoxon in presence of other OPs, for example fenitrothion, ediphenphos, and ethyl-paraoxon. The inhibition rate for fenitrothion, ediphenphos, and ethyl-paraoxon is 17.6%, 23.2%, and,

51.7% respectively, all lower than paraoxon, which ensures good biosensor selectivity for paraoxon. Sensor exhibited 87.93% and 111.02% recovery for paraoxon in pear and cucumber samples with 1.08% to 6.37% relative standard deviations (RSDs) value.

Electrode	**Analyte**	**LOD**	**Detection range**	**Ref.**
$Ru(bpy)_3^2$/ $Ti_3C_2T_x$	Label free single nucleotide mismatch	5nM		29
Nafion/ $Ti_3C_2T_x$	Dopamine	3nM	0.015 to 10 micro molar	30
DNA nanostructure/ $Ti_3C_2T_x$	Gliotoxin	5pM	5pM to 10nM	31
Hb/ Ti_3C_2MXene	Nitride	0.12 μM	0.5 to 11800 μM	32
$Ti_3C_2F_x$	H_2O_2	0.7nM		33
Pt NPs/ $Ti_3C_2T_x$ /GCE	H_2O_2	448nM		34
MXene/GCPE	Adrenaline	9.5nM		35
MnO2/Mn3O4/ Ti_3C_2 MXene/Au NPs	Methamidophos(pesticide)	1.34×10^{-13} M	10^{-12} M to 10^{-6} M	36
PPy@ $Ti_3C_2T_x$ /PMo12	Osteopontin	0.98 fg mL^{-1}	0.05 pg $mL^{-1}$to 10.0 ng mL^{-1}	38
Nafion/ lamellar $Ti_3C_2T_x$/GCE	Bromate (BrO3)	41nM	50 nM to 5 μM	39
W18O49/$Ti_3C_2T_x$	Acetone	170 ppb	11.6 to 20 ppm	40
Ti_3C_2-MWCNTs/GCE	catechol (CT) and hydroquinone (HQ)	6.6 nM (CT)and 3.9 nM (HQ)	2 to 150 μM	41
AChE/Ag@ $Ti_3C_2T_x$	Malathion (organophosphate pesticides)		10^{-14} to 10^{-8} M	42
GOx/Au/MXene/Nafion/GCE	Glucose	5.9μM	0.1 to 18 mM	43
$Ti_3C_2T_x$ /Pd NPs/GCE	L-cysteine (L-Cys)	0.14 mM	0.5 to 10 mM	44
TiO2/$Ti_3C_2T_x$	Ammonia gas	0.5 ppm	2-10 ppm	45
$Ti_3C_2T_x$ /Au-Pd NPs	organophosphorous pesticides	1.75 ng L^{-1}	0.1 to 1000 μg L^{-1}	46
cDNA-Fc/MXene/Apt/Au/GCE aptasensor	Mucin1	0.33 pM	1.0 pM to 10 μM	48

ECLprobe/exosome/Apt/ILs/SiO_2 NU's/GCE	Exosome	37 particle/μL	$.1\times10^2$ to 1.1×10^7 particle/μL	49
16SrDNA/Ti_3C_2	Mycobacterium tuberculosis	20CFUml^{-1}		50
MXene/MWCNT's/chit/GCE	IFO, AOCP, DOM, and SUM	0.00031, 0.00028, 0.00034, and 0.00042 μM	0.0011–1.0, 0.0042–7.1, 0.0046–7.3, and 0.0033–61 μM	54
BiNPs/Ti_3C_2/GCE	Pb, Cd	10.8 nm, 12.4 nm		56

Conclusion and future outlook

For the fabrication of sensors, Mxene is a new material. Since the discovery of mxene in 2011, due to its unique properties such as layered morphology, excellent metallic conductive, simple functionalization and catalytic properties, it has greatly attracted the interest of the scientific community. Some of its properties like large surface area and high compatibility are very important for designing advance nanohybrid systems with bio receptors like aptamer, antigen-antibody, proteins, enzyme and whole cells which can permit the easy immobilization of different bio-molecules on its surface which serve as sensitive detection interface. Because of exceptional structural, physical and chemical properties, mxene considered as best option as compare to other 2D materials and has potential to overcome the drawbacks of other 2D materials. The electrochemical performance of mxene is higher as compared to other 2D materials, such as graphene and MoS2. In this study, we addressed the new synthesis and surface functionalization techniques that are most useful in mass manufacturing. The applications of mxene based biosensors for the identification of environmental toxins, therapeutic agents and clinical biomarkers have also been summarized in this study. The general electrochemical properties such as detection limit, sensitivity, detection range and reproducibility of results are effectively discussed in this review. After a literature survey it was discovered that the electrochemical (bio) sensor based on maxene were adequately used for the identification of various analyte. In particular, mxene based electrochemical sensor for environmental contaminants are very useful because they exhibit detection limit in picomolar to femtomolar range that is much superior to ordinary strategies, for example chromatography and spectroscopy. Also the development of mxene based electrochemical gas sensors will contribute incredibly to different medical care diagnostics and ecological applications. However reports show that sensors for pharmaceutical formulation are limited and need more attention. In literature titanium carbide is the main mxene investigated in sensing field. The other transition metal based electrochemical are extremely uncommon. Therefore considerable scientific efforts are needed to utilize other transition metal based mxene. MXene has a promising future as a delicate electrochemical detection tool for a wide spectrum of analytics.

REFERENCES

1. Tan, C., Cao, X., Wu, X. J., He, Q., Yang, J., Zhang, X., … Zhang, H. (2017). Recent Advances in Ultrathin Two-Dimensional Nanomaterials. *Chemical Reviews*, *117*(9), 6225–6331. https://doi.org/10.1021/acs.chemrev.6b00558
2. Cai, X., Luo, Y., Liu, B., & Cheng, H. M. (2018). Preparation of 2D material dispersions and their applications. *Chemical Society Reviews*, *47*(16), 6224–6266. https://doi.org/10.1039/c8cs00254a
3. Xu, B., Zhi, C., & Shi, P. (2020). *Latest advances in MXene biosensors Journal of Physics : Materials OPEN ACCESS Latest advances in MXene biosensors*.
4. Sinha, A., Zhao, H., Huang, Y., Lu, X., Chen, J., & Jain, R. (2018). SC. *Trends in Analytical Chemistry*. https://doi.org/10.1016/j.trac.2018.05.021
5. Wang, H., Wu, Y., Yuan, X., Zeng, G., Zhou, J., Wang, X., & Chew, J. W. (2018). Clay-Inspired MXene-Based Electrochemical Devices and Photo-Electrocatalyst: State-of-the-Art Progresses and Challenges. *Advanced Materials*, *30*(12), 1–28. https://doi.org/10.1002/adma.201704561
6. Kim, H., Wang, Z., & Alshareef, H. N. (2019). MXetronics: Electronic and photonic applications of MXenes. *Nano Energy*, *60*(March), 179–197. https://doi.org/10.1016/j.nanoen.2019.03.020
7. Zhang, Y., Wang, L., Zhang, N., & Zhou, Z. (2018). Adsorptive environmental applications of MXene nanomaterials: A review. *RSC Advances*, *8*(36), 19895–19905. https://doi.org/10.1039/c8ra03077d
8. Sinha, A., Zhao, H., Huang, Y., Lu, X., Chen, J., & Jain, R. (2018). SC. *Trends in Analytical Chemistry*. https://doi.org/10.1016/j.trac.2018.05.021
9. Kalambate, P. K., Biradar, M. R., Karna, S. P., & Srivastava, A. K. (2015). Adsorptive stripping differential pulse voltammetry determination of rivastigmine at graphene nanosheet-gold nanoparticle/carbon paste electrode. *Journal of Electroanalytical Chemistry*, *757*, 150–158. https://doi.org/10.1016/j.jelechem.2015.09.027
10. Kalambate, P. K., Rawool, C. R., & Srivastava, A. K. (2016). Voltammetric determination of pyrazinamide at graphene-zinc oxide nanocomposite modified carbon paste electrode employing differential pulse voltammetry. *Sensors and Actuators, B: Chemical*, *237*, 196–205. https://doi.org/10.1016/j.snb.2016.06.019
11. Huang, K., Li, Z., Lin, J., Han, G., & Huang, P. (2018). Two-dimensional transition metal carbides and nitrides (MXenes) for biomedical applications. *Chemical Society Reviews*, *47*(14), 5109–5124. https://doi.org/10.1039/c7cs00838d
12. Khazaei, M., Arai, M., Sasaki, T., Chung, C. Y., Venkataramanan, N. S., Estili, M., … Kawazoe, Y. (2013). Novel electronic and magnetic properties of two-dimensional transition metal carbides and nitrides. *Advanced Functional Materials*, *23*(17), 2185–2192. https://doi.org/10.1002/adfm.201202502
13. Kurtoglu, M., Naguib, M., Gogotsi, Y., & Barsoum, M. W. (2012). First principles study of two-dimensional early transition metal carbides. *MRS Communications*, *2*(4), 133–137. https://doi.org/10.1557/mrc.2012.25
14. Srivastava, P., Mishra, A., Mizuseki, H., Lee, K. R., & Singh, A. K. (2016). Mechanistic Insight into the Chemical Exfoliation and Functionalization of Ti3C2 MXene. *ACS Applied Materials and Interfaces*, *8*(36), 24256–24264. https://doi.org/10.1021/acsami.6b08413
15. Sang, X., Xie, Y., Lin, M. W., Alhabeb, M., Van Aken, K. L., Gogotsi, Y., … Unocic, R. R. (2016). Atomic defects in monolayer titanium carbide (Ti3C2Tx) MXene. *ACS Nano*, *10*(10), 9193–9200. https://doi.org/10.1021/acsnano.6b05240

16. Ghidiu, M., Lukatskaya, M. R., Zhao, M. Q., Gogotsi, Y., & Barsoum, M. W. (2015). Conductive two-dimensional titanium carbide "clay" with high volumetric capacitance. *Nature*, *516*(7529), 78–81. https://doi.org/10.1038/nature13970
17. M. Naguib, V.N. Mochalin, M.W. Barsoum, Y. Gogotsi, (2014) MXenes: a new family of two- dimensional materials, Adv. Mater., 26 992–1005.
18. M. Naguib, O. Mashtalir, J. Carle, V. Presser, J. Lu, L. Hultman, Y. Gogotsi, M.W. Barsoum, (2012)Two dimensional transition metal carbides, ACS Nano, 6 1322-1331.
19. B. Anasori, Y. Xie, M. Beidaghi, J. Lu, B.C. Hosler, L. Hultman, P.R.C. Kent, Y. Gogotsi, M.W. Barsoum, (2015) Two dimensional, ordered, double transition metals carbides (MXenes), ACS Nano, 9 9507-9516.
20. Mashtalir, O., Naguib, M., Mochalin, V. N., Dall'Agnese, Y., Heon, M., Barsoum, M. W., & Gogotsi, Y. (2013). Intercalation and delamination of layered carbides and carbonitrides. *Nature Communications*, *4*, 1–7. https://doi.org/10.1038/ncomms2664
21. Mashtalir, O., Lukatskaya, M. R., Zhao, M. Q., Barsoum, M. W., & Gogotsi, Y. (2015). Amine-assisted delamination of Nb2C MXene for li-ion energy storage devices. *Advanced Materials*, *27*(23), 3501–3506. https://doi.org/10.1002/adma.201500604
22. Halim, J., Kota, S., Lukatskaya, M. R., Naguib, M., Zhao, M. Q., Moon, E. J., … Barsoum, M. W. (2016). Synthesis and Characterization of 2D Molybdenum Carbide (MXene). *Advanced Functional Materials*, *26*(18), 3118–3127. https://doi.org/10.1002/adfm.201505328
23. Alhabeb, M., Maleski, K., Mathis, T. S., Sarycheva, A., Hatter, C. B., Uzun, S., … Gogotsi, Y. (2018). Selective Etching of Silicon from Ti 3 SiC 2 (MAX) To Obtain 2D Titanium Carbide (MXene) . *Angewandte Chemie*, *130*(19), 5542–5546. https://doi.org/10.1002/ange.201802232
24. Overbury, S. H., Kolesnikov, A. I., Brown, G. M., Zhang, Z., Nair, G. S., Sacci, R. L., … Naguib, M. (2018). Complexity of Intercalation in MXenes: Destabilization of Urea by Two-Dimensional Titanium Carbide. *Journal of the American Chemical Society*, *140*(32), 10305–10314. https://doi.org/10.1021/jacs.8b05913
25. J. Zhu, E. Ha, G. Zhao, Y. Zhou, D. Huang, G. Yue, L. Hu, N. Sun, Y. Wang, L.Y.S. Lee, C. Xu, K.Y. Wong, D. Astruc, P. Zhao, (2017) Recent advance in MXenes: A promising 2D material for catalysis, sensor and chemical adsorption, Coord. Chem. Rev., 352 306-327.
26. V.M.H. Ng, H. Huang, K. Zhou, P.S. Lee, W. Que, J.Z. Xu, L.B. Kong, (2017) Recent progress in layered transition metal carbides and/or nitrides (MXenes) and their composites: synthesis and applications, J. Mater. Chem. A, 5 3039-3068.
27. J.C. Lei, X. Zhang, Z. Zhou, (2015) Recent advances in mxene: preparation, properties and applications, Front. Phys., 10 107303-107311.
28. M. Khazaei, M. Arai, T. Sasaki, C.Y. Chung, N.S. Venkataramanan, M. Estili, Y. Sakka, Y. Kawazoe, (2013) Novel electronic and magnetic properties of two-dimensional transition metal carbides and nitrides, Adv. Funct. Mater., 23 2185-2192.
29. Fang, Y., Yang, X., Chen, T., Xu, G., Liu, M., Liu, J., & Xu, Y. (2018) Two dimensional titanium carbide (MXene)-based solid-state electrochemiluminescent sensor for label-free single-nucleotide mismatch discrimination in human urine. Sensors and Actuators, B: Chemical, 263, 400–407.
30. Shahzad, F., Iqbal, A., Zaidi, S. A., Hwang, S. W., & Koo, C. M. (2019) Nafion-stabilized two-dimensional transition metal carbide (Ti3C2Tx MXene) as a high-performance electrochemical sensor for neurotransmitter. Journal of Industrial and Engineering Chemistry.

31. Wang, H., Li, H., Huang, Y., Xiong, M., Wang, F., & Li, C. (2019) A label-free electrochemical biosensor for highly sensitive detection of gliotoxin based on DNA nanostructure/MXene nanocomplexes. Biosensors and Bioelectronics, 142, 111531.
32. Liu, H., Duan, C., Yang, C., Shen, W., Wang, F., & Zhu, Z. (2015) A novel nitrite biosensor based on the direct electrochemistry of hemoglobin immobilized on MXene. In Sensors and Actuators, B: Chemical (Vol. 218).
33. Lorencova, L., Bertok, T., Dosekova, E., Holazova, A., Paprckova, D., Vikartovska, A., Tkac, J. (2017) Electrochemical performance of Ti3C2Tx MXene in aqueous media: towards ultrasensitive H2O2 sensing. Electrochimica Acta, 235, 471–479.
34. Lorencova, L., Bertok, T., Filip, J., Jerigova, M., Velic, D., Kasak, P., … Tkac, J. (2018) Highly stable Ti3C2Tx (MXene)/Pt nanoparticles-modified glassy carbon electrode for H2O2 and small molecules sensing applications. Sensors and Actuators, B: Chemical, 263, 360–368.
35. Shankar, S. S., Shereema, R. M., & Rakhi, R. B. (2018) Electrochemical Determination of Adrenaline Using MXene/Graphite Composite Paste Electrodes. ACS Applied Materials and Interfaces, 10(50), 43343–43351.
36. Song, D., Jiang, X., Li, Y., Lu, X., Luan, S., Wang, Y., Gao, F. (2019) Metal−organic frameworks-derived MnO 2 /Mn 3 O 4 microcuboids with hierarchically ordered nanosheets and Ti 3 C 2 MXene/Au NPs composites for electrochemical pesticide detection. Journal of Hazardous Materials, 367–376.
37. Wu, D., Wu, M., Yang, J., Zhang, H., Xie, K., Lin, C. Te, … Fu, L. (2019) Delaminated Ti3C2Tx (MXene) for electrochemical carbendazim sensing. Materials Letters, 236, 412–415.
38. Zhou, S., Gu, C., Li, Z., Yang, L., He, L., Wang, M., Zhang, Z. (2019) Ti3C2Tx MXene and polyoxometalate nanohybrid embedded with polypyrrole: Ultra-sensitive platform for the detection of osteopontin. Applied Surface Science, 498(August), 143889.
39. Pandey, R. P., Rasool, K., Rasheed, P. A., & Mahmoud, K. A. (2018) Reductive Sequestration of Toxic Bromate from Drinking Water using Lamellar Two-Dimensional Ti3C2TX (MXene). ACS Sustainable Chemistry and Engineering, 6(6), 7910–7917.
40. Sun, S., Wang, M., Chang, X., Jiang, Y., Zhang, D., Wang, D., Lei, Y. (2020) W18O49/Ti3C2Tx Mxene nanocomposites for highly sensitive acetone gas sensor with low detection limit. Sensors and Actuators, B: Chemical, 304, 127274.
41. Huang, R., Chen, S., Yu, J., & Jiang, X. (2019) Self-assembled Ti3C2 /MWCNTs nanocomposites modified glassy carbon electrode for electrochemical simultaneous detection of hydroquinone and catechol. Ecotoxicology and Environmental Safety, 184, 109619.
42. Jiang, Y., Zhang, X., Pei, L., Yue, S., Ma, L., Zhou, L., Gao, J. (2018) Silver nanoparticles modified two-dimensional transition metal carbides as nanocarriers to fabricate acetycholinesterase-based electrochemical biosensor. Chemical Engineering Journal, 339, 547–556.
43. Rakhi, R. B., Nayuk, P., Xia, C., & Alshareef, H. N. (2016) Novel amperometric glucose biosensor based on MXene nanocomposite. Scientific Reports, 6, 1–9.
44. Rasheed, P. A., Pandey, R. P., Jabbar, K. A., Ponraj, J., & Mahmoud, K. A. (2019) Sensitive electrochemical detection of l -cysteine based on a highly stable Pd@Ti 3 C 2 T x (MXene) nanocomposite modified glassy carbon electrode . Analytical Methods, 11(30), 3851–3856.

45. Tai, H., Duan, Z., He, Z., Li, X., Xu, J., Liu, B., & Jiang, Y. (2019) Enhanced ammonia response of Ti3C2T nanosheets supported by TiO2 nanoparticles at room temperature. Sensors and Actuators B: Chemical, 298, 126874.
46. Zhao, F., Yao, Y., Jiang, C., Shao, Y., Barceló, D., Ying, Y., & Ping, J. (2020) Self-reduction bimetallic nanoparticles on ultrathin MXene nanosheets as functional platform for pesticide sensing. Journal of Hazardous Materials, 384, 121358.
47. Liu, X., Li, P., Mao, C., Niu, H., Song, J., & Jin, B. (2018). Enhanced Photoelectrochemical Sensing for MUC1 Detection Based on TiO2/CdS:Eu/CdS Cosensitized Structure. *Sensors & Actuators: B. Chemical*. https://doi.org/10.1016/j.snb.2018.07.140
48. Wang, H., Sun, J., Lu, L., Yang, X., Xia, J., & Zhang, F. (2019). Competitive electrochemical aptasensor based on a cDNA-ferrocene/MXene probe for detection of breast cancer marker Mucin1. *Analytica Chimica Acta*. https://doi.org/10.1016/j.aca.2019.10.003
49. Fang, D., Zhao, D., Zhang, S., Huang, Y., Dai, H., & Lin, Y. (2020). Sensors and Actuators B : Chemical Black phosphorus quantum dots functionalized MXenes as the enhanced dual-mode probe for exosomes sensing. *Sensors & Actuators: B. Chemical*, *305*(December 2019), 127544. https://doi.org/10.1016/j.snb.2019.127544
50. Zhang, J., Li, Y., Duan, S., & He, F. (2020). Analytica Chimica Acta Highly electrically conductive two-dimensional Ti 3 C 2 Mxenes-based 16S rDNA electrochemical sensor for detecting Mycobacterium tuberculosis. *Analytica Chimica Acta*, *1123*, 9–17. https://doi.org/10.1016/j.aca.2020.05.013
51. Sun, S., Wang, M., Chang, X., Jiang, Y., Zhang, D., Wang, D., … Lei, Y. (2019). Jo ur na l P of. *Sensors & Actuators: B. Chemical*, 127274. https://doi.org/10.1016/j.snb.2019.127274
52. Kalambate, P. K., Huang, Z., Li, Y., Shen, Y., Xie, M., Huang, Y., & Srivastava, A. K. (2019). Trends in Analytical Chemistry Core @ shell nanomaterials based sensing devices : A review. *Trends in Analytical Chemistry*, *115*, 147–161. https://doi.org/10.1016/j.trac.2019.04.002
53. Sinha, A., Zhao, H., Huang, Y., Lu, X., Chen, J., & Jain, R. (2018). SC. *Trends in Analytical Chemistry*. https://doi.org/10.1016/j.trac.2018.05.021
54. Kalambate, P. K. (2020). *An electrochemical sensor for ifosfamide , acetaminophen , domperidone , and sumatriptan based on self-assembled MXene / MWCNT / chitosan nanocomposite thin film*.
55. He, Y., Zhou, L., Liu, G., Jiang, Y., & Gao, J. (2020). *Preparation and Application of Bismuth / MXene Nano-Composite as Electrochemical Sensor for Heavy Metal Ions Detection*.
56. Tchounwou, P. B., Yedjou, C. G., Patlolla, A. K., & Sutton, D. J. (n.d.). *Heavy Metal Toxicity and the Environment*. https://doi.org/10.1007/978-3-7643-8340-4
57. Cui, L., Wu, J., & Ju, H. (2015). Biosensors and Bioelectronics Electrochemical sensing of heavy metal ions with inorganic , organic and bio-materials. *Biosensors and Bioelectronic*, *63*, 276–286. https://doi.org/10.1016/j.bios.2014.07.052
58. Afkhami, A., Soltani-felehgari, F., Madrakian, T., & Ghaedi, H. (2013). Analytica Chimica Acta Fabrication and application of a new modified electrochemical sensor using nano-silica and a newly synthesized Schiff base for simultaneous determination of Cd 2 + , Cu 2 + and Hg 2 + ions in water and some foodstuff samples. *Analytica Chimica Acta*, *771*, 21–30. https://doi.org/10.1016/j.aca.2013.02.031
59. Gong, T., Liu, J., Liu, X., Liu, J., Xiang, J., & Wu, Y. (2016). A sensitive and selective sensing platform based on CdTe QDs in the presence of L-cysteine for

detection of silver, mercury and copper ions in water and various drinks. *Food Chemistry*. https://doi.org/10.1016/j.foodchem.2016.06.091

60. Gros, P. (2014). *Electrochemical sensors and devices for heavy metals assay in water : the French groups ' contribution*. *2*(April), 1–24. https://doi.org/10.3389/fchem.2014.00019
61. Aragay, G., & Merkoc, A. (2012). *Electrochimica Acta Nanomaterials application in electrochemical detection of heavy metals*. *84*, 49–61. https://doi.org/10.1016/j.electacta.2012.04.044
62. Nejdl, L., Kudr, J., Cihalova, K., Chudobova, D., Zurek, M., Zalud, L., … Kizek, R. (2014). *Remote-controlled robotic platform ORPHEUS as a new tool for detection*. 1–13. https://doi.org/10.1002/elps.201300576
63. Nanoparticles, Z. S. (2013). *Behaviour of Zinc Complexes and Zinc Sulphide Nanoparticles Revealed by Using Screen Printed Electrodes and Spectrometry*. (Ii), 14417–14437. https://doi.org/10.3390/s131114417
64. Locatelli, C., & Melucci, D. (2013). *Voltammetric method for ultra-trace determination of total mercury and toxic metals in vegetables . Comparison with spectroscopy*. *11*(5). https://doi.org/10.2478/s11532-013-0221-8
65. Huang, R., Chen, S., Yu, J., & Jiang, X. (2019). Ecotoxicology and Environmental Safety Self-assembled Ti 3 C 2 / MWCNTs nanocomposites modi fi ed glassy carbon electrode for electrochemical simultaneous detection of hydroquinone and catechol. *Ecotoxicology and Environmental Safety*, *184*(July), 109619. https://doi.org/10.1016/j.ecoenv.2019.109619
66. Zhao, F., Yao, Y., Jiang, C., Shao, Y., Barcel, D., Ying, Y., & Ping, J. (2019). Jo ur l P re of. *Journal of Hazardous Materials*, 121358. https://doi.org/10.1016/j.jhazmat.2019.121358
67. Kaur, N., & Prabhakar, N. (2017). Current scenario in organophosphates detection using electrochemical biosensors. *Trends in Analytical Chemistry*. https://doi.org/10.1016/j.trac.2017.04.012
68. Zhao, F., Wu, J., Ying, Y., She, Y., Wang, J., & Ping, J. (2018). Carbon nanomaterial-enabled pesticide biosensors: design strategy, biosensing mechanism, and practical application. *Trends in Analytical Chemistry*. https://doi.org/10.1016/j.trac.2018.06.017
69. Tang, W., Yang, J., Wang, F., & Wang, J. (2019). Analytica Chimica Acta Thiocholine-triggered reaction in personal glucose meters for portable quantitative detection of organophosphorus pesticide. *Analytica Chimica Acta*, *1060*, 97–102. https://doi.org/10.1016/j.aca.2019.01.051
70. Kumar, J. V., Karthik, R., Chen, S., Natarajan, K., Karuppiah, C., Yang, C., & Muthuraj, V. (2018). *Energy , Environmental , and Catalysis Applications 3D Flower-Like Gadolinium Molybdate Catalyst for Efficient Detection and Degradation of Organophosphate Pesticide (Fenitrothion) 3D Flower-Like Gadolinium Molybdate Catalyst for Efficient Detection and Electroanalysis and Bioelectrochemistry Lab , Department of Chemical Engineering and*. https://doi.org/10.1021/acsami.8b00625
71. Zhao, F., Yao, Y., Li, X., Lan, L., Jiang, C., & Ping, J. (2018). *Metallic Transition Metal Dichalcogenide Nanosheets as an Effective and Biocompatible Transducer for Electrochemical Detection of Pesticide Metallic Transition Metal Dichalcogenide Nanosheets as an Effective and Biocompatible Transducer for Electrochemical Detection of Pesticide*. https://doi.org/10.1021/acs.analchem.8b03250